MAPPING CLOUDS MICROPHYSICS WITH OMEGA/MEX.

J.-B. Madeleine[1,2], J.-P. Bibring[1], B. Gondet[1], F. Forget[2], F. Montmessin[3], A. Spiga[2], D. Jouglet[1], M. Vincendon[1], Y. Langevin[1], F. Poulet[1], B. Schmitt[4].

[1]IAS, Orsay, France. [2]Laboratoire de Météorologie Dynamique, Institut Pierre Simon Laplace, Paris, France. [3]Service d'Aéronomie, Institut Pierre Simon Laplace, Paris, France. [4]Laboratoire de Planétologie de Grenoble, France.

jbmlmd@lmd.jussieu.fr

Summary

Near-IR hyper-spectral imaging of clouds is made possible by the OMEGA (Observatoire pour la Minéralogie, l'Eau, les Glaces et l'Activité) instrument [1]. Image cubes (x,λ,y) of kilometer-scale spatial resolution with wavelengths spanning 0.35 to 5.1 µm are used to 1) detect clouds and map their microphysics using RGB compositions and 2) retrieve ice crystals size and cloud opacity.

Both methods are described in the lower panel, and meteorological applications are presented below. Visible images and false color maps are used along with a framework (fig. **1.**) which gives an assessment of the particle size and cloud opacity corresponding to a given color. Local retrieval of these parameters is also achieved. Improvements of the model are underway to take into account parameter uncertainties and retrieve ice crystals size and cloud opacity over an entire orbit.

Meteorological applications

Polar regions : The different response of the 1.5 µm and 3 µm absorption bands to the ice particle size [2] is used in RGB compositions to distinguish between surface frost and clouds, as illustrated on image **a.** Seasonal frost appears in magenta around 76°N, and on the rim of a crater. Spring clouds appear in blue at the margin of these deposits (see the spectra of fig. **b.**). Kilometer-scale variations in clouds microphysics are clearly seen, for exemple on image **c.**

Equatorial Cloud Belt : Evolution of the Aphelion Cloud Belt is characterized by an early period of cloud development (hazes and fibrous clouds) during L_s 45-130°, followed by convective cloud formation during L_s 80-130° [3,4]. Examples of these clouds are shown in figures **d. e. f.**, and an assessment of their microphysics using the framework of fig. **1.** gives intermediate particle size (type **II.** on fig.**1.**) for thick hazes (fig. **d.** and **f.**) and large crystal size (type **III.** on fig.**1.**) for convective clouds (fig. **e.** ; RGB composition is all covered by dark blue tones, and not shown). Inversion results (see fig. **e.** and **f.**) are consistent with TES EPF observations [6] and GCM results [12], but effective radius can reach 6 µm for the convective clouds of fig. **e.**

Polar regions

a. Water-ice frost and clouds in the northern polar region.

ORB3064_3 (75.1N,168.2W) Ls 59.4

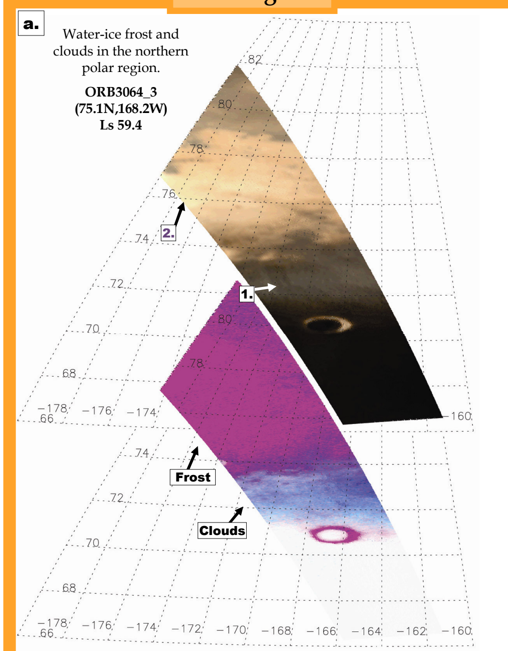

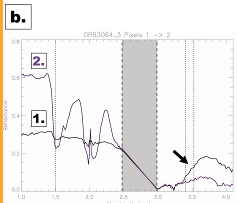

b. Spectra of clouds (1) and surface ice (2) measured during orbit **a.** 3.4 µm signature is indicated by an arrow.

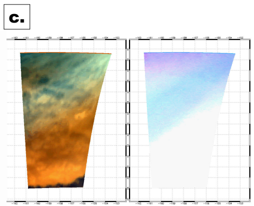

c. Cloud curtain in Vastitas Borealis.

ORB2388_6 (44.6N,161.3W) - Ls 328.2

Equatorial Cloud Belt

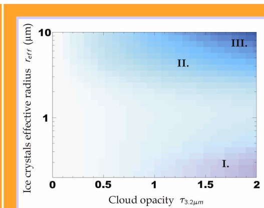

I. Fine crystals $r_e < 0.5$ µm ; $\tau_c > 1$

II. Intermediate crystals $r_e \sim 3$ µm ; $0.5 < \tau_c < 2$

III. Large crystals $r_e > 4$ µm ; $\tau_c > 1$

Fig. 1. : Framework for reading of RGB compositions. Colors are reproduced by the radiative transfer model, with effective radius r_e on y-axis and cloud opacity τ_c on x-axis.

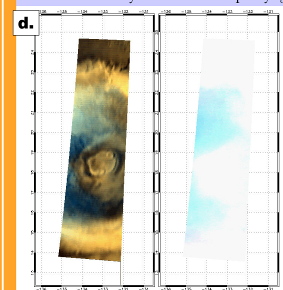

d. Clouds over Olympus Mons (upper panel) and Ascraeus Mons (lower panel).

ORB3635_3 (19.0N,133.3W) - Ls 131.3
ORB3664_4 (6.1N,105.3W) - Ls 135.2

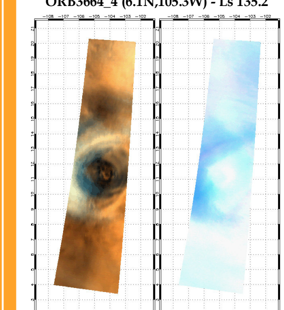

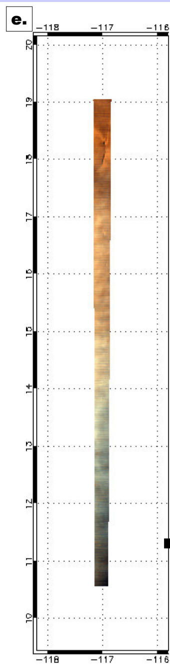

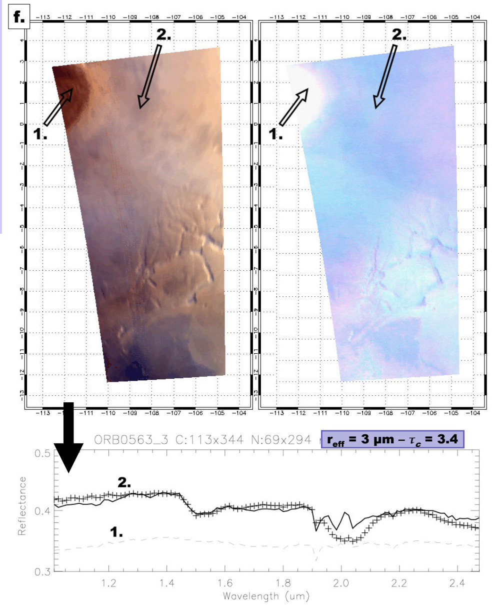

f. Thick haze near Pavonis Mons (upper panel) and model results (lower panel).

ORB0563_3 (4.1S,108.0W) - Ls 53.6.

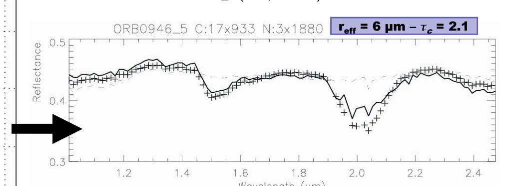

e. Convective clouds over the Tharsis plateau (on the left) and model results (above).

ORB0946_5 (21.8N,117.0W) - Ls 100.7.

1) Introduction

Near-IR hyper-spectral imaging of clouds is currently used on Earth as a powerful meteorological tool, and this technique is made possible on Mars by the OMEGA (Observatoire pour la Minéralogie, l'Eau, les Glaces et l'Activité, [1]) imaging spectrometer. Past analysis of clouds has been done in the visible range with Mariner 9 and Viking Orbiter [3], and more recently in the visible (MOC images [4]) and thermal infrared (TES, 6 to 50 µm [5,6]) with Mars Global Surveyor.

Bridging the gap, OMEGA data are spectral image cubes (x,λ,y) of the atmosphere and the surface both in the visible and near infrared, spanning 0.35 to 5.1 µm with a spectral sampling of 0.013-0.020 µm and kilometer-scale spatial resolution. Spectral range includes water ice absorptions at 1.25, 1.5, 2 and 3 µm that can be used to detect water-ice clouds and derive their microphysical properties.

Analyzing the kilometer-scale microphysics of clouds on Mars is key to understanding their formation, their role in the water cycle and radiative transfer of the planet, their interaction with the dust cycle, and can provide major insights into the fundamental physics of nucleation.

2) Cloud cover mapping

To first detect and map the cloud cover, 1.5 and 3 µm water ice absorption bands are visualized using RGB composition :

- the **red** is proportional to the slope at the edge of the 3 µm H_2O vibration band (3.4/3.525 µm criterion defined in [2]) ;
- the **green** is proportional to the depth of the 1.5 µm water-ice absorption band (used in [7]) ;
- the **blue** is held constant.

Correlated increase of the 1.5 µm absorption depth and 3.4 µm slope reveals the formation of water ice clouds, and appears in blue. On the contrary, large 1.5 µm absorption depth and drop of the 3.4 µm slope are typical of surface grains larger than 10 µm which appear in magenta, allowing us to distinguish between surface ice and clouds (see image **a.**).

3) Cloud microphysical properties

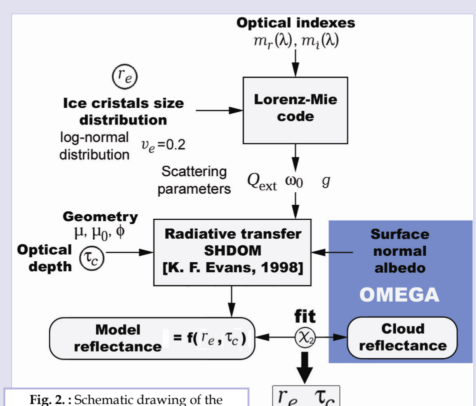

Fig. 2. : Schematic drawing of the water-ice crystals size r_e and clouds optical depth τ_c retrieval method.

Cloud optical depth and particle size can be retrieved at a given point using an inversion method presented on figure **2.** The model minimizes the difference between a simulated reflectance and the observed cloud reflectance by using a downhill simplex method and a least-squares criterion. The free parameters are the optical depth of the cloud at 3.2 µm τ_c and the water ice crystal effective radius r_e.

These two parameters are fitted during the inversion by calculating the radiative transfer through a single-layer atmosphere using the Spherical Harmonics Discrete Ordinate Method [8]. Scattering parameters are given by a Lorenz-Mie code which uses the recent ice optical constants at 180K of Grundy & Schmitt [9], and assumes that the ice crystals are spherical and follow a unimodal log-normal distribution (effective variance of 0.2). A spectrum of the same region, free of any clouds, must be used as a surface boundary condition of the model. This spectrum must be carefully chosen through a "man-in-the-loop" method, in order to make sure that the surface geology, the atmospheric dust opacity and the viewing geometry are similar to what is found for the analyzed cloudy pixel.

The radiative transfer model can also reproduce the behaviour of the 1.5 µm absorption band and 3.4 µm slope to generate a framework given in figure **1.** This framework is a first guiding tool for reading RGB compositions and assessing cloud particle size and opacity. Indeed, automatic inversion of the two microphysical parameters (r_e,τ_c) over an entire orbit is still a challenge that has to be addressed.

4) Ongoing improvements and analyses

Improvements of the inversion model are underway to take into account the retrieval uncertainties, the radiative effect of atmospheric dust [10] and ice nucleation on mineral dust cores, the contribution of the 3 µm hydration band of surface dust [11], and to quantitatively map the microphysical properties over an entire orbit.

Final results from the inversion model will be compared to the water cycle simulated by the LMD/GCM (see [12] and poster [13]), and regional cloud structures will be interpreted with the help of the new LMD mesoscale model (poster [14]).

References

[1] Bibring, J.-P. et al. (2005), *Science 307*. [2] Langevin, Y. et al. (2006), *JGR 112:E8*. [3] Kahn, R. (1984), *JGR 89*. [4] Wang, H. and Ingersoll, A. P. (2002), *JGR 107*. [5] Smith, M. D. (2004), *Icarus 167*. [6] Clancy, R. T. et al. (2003), *JGR 108*. [7] Gondet, B. et al. (2006), *AGU Abs. #P14A-02*. [8] Evans, K. F. (1998), *J. Atmos. Sci. 55*. [9] Grundy, W. M. and Schmitt, B. (1998), *JGR 103*. [10] Vincendon, M. et al. (2007), *JGR 112:E11*. [11] Jouglet, D. et al. (2007), *JGR 112:E11*. [12] Montmessin, F. et al. (2004), *JGR 109:E18*. [13] Millour, E. et al., *The new Mars Climate Database*, poster #1118452. [14] Spiga, A. et al., *A new mesoscale model for the Martian atmosphere*, #1119867.